Published by Avanti Publishers

Global Journal of Earth Science and Engineering

ISSN (online): 2409-5710

Groundwater Classification by Using Fourier Analysis

Mohamed A. Khalil*

Conservation and Survey Division, School of Natural Resources, University of Nebraska-Lincoln, USA

ARTICLE INFO

Article Type: Research Article

Keywords:
Stiff diagrams
Andrews plots
Fourier analysis
Groundwater statistics
Quaternary and Pre-Quaternary aquifers

Timeline:
Received: April 18, 2022
Accepted: August 03, 2022
Published: August 22, 2022

Citation: Khalil MA. Groundwater Classification by Using Fourier Analysis. Glob J Earth Sci Eng. 2022; 9: 65-73.

DOI: https://doi.org/10.15377/2409-5710.2022.09.5

ABSTRACT

The article illustrates a statistical technique for the visual representation of geochemical data. Quaternary and Pre-Quaternary groundwater samples from Northern Sinai Peninsula, Egypt, were interpreted statistically using Andrews plots, which use Fourier analysis to transform and represent a set of multivariate data by a waveform pattern. The resulting waveform patterns were classified into low, middle, and high amplitudes, following up the increase in the total dissolved solids of the samples. Comparison with the traditional hydrochemical polygonal Stiff diagrams resulted in a complete matching. The proposed mixing between the Quaternary and Pre-Quaternary aquifers has been proved via the similarity of waveform patterns of the mixed water. The application of Andrews plots is investigated by comparison with the Stiff conventional diagrams. The correlation between different amplitudes and the TDS value of every sample indicates that the amplitude increases with the increase in the salinity.

*Corresponding Author
Email: maboushanab2@unl.edu
Tel: +(1) 406 479 4073

1. Introduction

Mixing between Quaternary and Pre-Quaternary groundwater in Delta Wadi El Arish, Northern Sinai, has been studied by many authors such as [5]. They suggested that the increase of Total Dissolved Solids (TDS) of the groundwater samples collected from the wells to the north of El Aish airport was attributed to the inflow of saline water into the Quaternary aquifer by vertical movement from the deep aquifer along the Lehfan fault. Gomaa [8] has referred to the Early Cretaceous sandstone aquifer as an important charging source of the shallower Quaternary aquifer. Khalil [12] established a detailed geophysical, hydrochemical, and isotope hydrological study to elucidate the source of high salinity groundwater in the delta of Wadi El Arish. His study revealed that the high salinity is attributed to the inflow of Pre-Quaternary high salinity evaporite dissolved water into the shallower fresh Quaternary groundwater forming a mixed zone to the east of El Arish city. The estimated radiocarbon age of groundwater samples in the mixed zone ranges from 900 to 8800 Y.B.P. Tritium dating refers to the mixing between modern to sub-modern or old age. The present study is an approach to classify groundwater samples and illustrate groundwater mixing using Andrews plots, which have recently achieved significant recognition in different areas. Andrews plots is a technique that uses Fourier analysis to transform and represent a set of multivariate data by a waveform pattern. The mathematical details of the method are discussed by [13]. Andrews plots have many applications in different areas, such as robust design [15], correspondence analysis techniques [10], uncertainty analysis [6], and classification techniques for Landsat images [3].

Geological and Hydrogeological Setting

The geological succession of the Northern Sinai coastal zone and the delta of Wadi El Arish are shown in table (**1**). The Quaternary aquifer consists of three hydraulically connected water-bearing formations (1) Holocene sand dune and Upper Pleistocene old beach sand, (2) Alluvium deposits, and (3) Lower Pleistocene calcareous sandstone (Kurkar). The TDS of the Quaternary aquifer ranges from 800 to 7000 ppm. The Quaternary aquifer is characterized by low potentiometric gradient, where the potentiometric surface ranges from +1.5 to -2 meters [9].

The Upper Cretaceous aquifer system consists mainly of chalky limestone and shale in the upper part (Senonian) and limestone, dolomite, dolomitic limestone, and marls in the lower part (Turonian and Cenomanian). The lower boundary of the Upper Cretaceous aquifer is a marly or shally aquiclude changing into calcareous sandstone toward the south. The upper boundary is the base of the overlying Tertiary Formation, which dominates the major part of central and northeastern Sinai. The total salinity of the Upper Cretaceous aquifer ranges from 1000 ppm in middle Sinai to 10.000 ppm in northern Sinai. The potentiometric surface map of the Upper Cretaceous aquifer ranges from +600m in the middle of Sinai to +50m in northern Sinai. The locations of the studied water samples in both Upper Cretaceous and Quaternary aquifers are shown in Figures (**1**) and (**2**), respectively. The hydrochemical data of the Upper Cretaceous and Quaternary aquifer (Table **2**) are collected from [1, 9, 14].

Interpretation

Collected water samples representing Quaternary and Upper Cretaceous aquifers are interpreted statistically using Andrews plots in association with the conventional polygonal Stiff diagram.

Andrews plotting is a technique that uses Fourier analysis to transform the results of multivariate data and represents a set of multivariate data by a waveform pattern [4]. Andrews plotting or curve is a way to visualize structure in high-dimensional data [7]. Anderson [2] suggested that a *P*-dimensional vector of measurements (*X1, X2 ...Xp*) be represented by the finite Fourier series as shown in equation (1).

$$f(t) = \frac{x_1}{\sqrt{2}} + x_2 \sin t + x_3 \cos t + x_4 \sin 2t + x_5 \cos 2t + \ldots\ldots\ldots\ldots\ldots\ldots\ldots, -\pi \leq t \geq \pi \quad (1)$$

Table 1: Geological succession of El-Arish-Rafah area, modified after different authors.

<table>
<tr><th colspan="3">Age</th><th colspan="3">Lithologic Description</th><th>Thickness (m)</th><th>Locality</th><th colspan="2">Geologic History and Environment</th></tr>
<tr><td rowspan="10">Quaternary</td><td rowspan="4" colspan="2">Holocene</td><td colspan="3">Sand dunes: -
Loose, fine to course, rounded to sub-rounded, well sorted quartz grains mixed with carbonates.</td><td>Variable</td><td>Covered almost the study area</td><td colspan="2">Aridity condition</td></tr>
<tr><td colspan="3">Modern beach deposits
Loose sand &hard sand cemented by calcium carbonates</td><td>Variable</td><td>El-Arish-Rafah coastal plain</td><td colspan="2">Formed under warm water condition</td></tr>
<tr><td colspan="3"><u>Holocene wadi filling:</u>
Loam, sand, clay, silt with calcareous materials (mud flats)</td><td>5-25</td><td>Channel of Wadi El-Arish</td><td rowspan="2" colspan="2">Wadi El-Arish lowered its level and formation of alluvial terraces</td></tr>
<tr><td colspan="3"><u>Salt marsh deposits:</u>
Evaporites mixed with detrital materials, eolian sand and clay.</td><td></td><td>Sabkhat El-Sheikh Zuwied</td></tr>
<tr><td rowspan="6">Pleistocene</td><td rowspan="4">U</td><td colspan="3"><u>Old beach deposits:</u>
Sands intercalated with clay &silt</td><td>10</td><td>Abu-Sagal and El-Sheikh Zuwied</td><td colspan="2"></td></tr>
<tr><td rowspan="3">Alluvial deposits</td><td>U</td><td>Medium to coarse grain sands and silt</td><td>13</td><td rowspan="3">Along Wadi El-Arish and its tributaries</td><td rowspan="2" colspan="2">Delta condition (formation of the present delta)</td></tr>
<tr><td>M</td><td>Sand and calcareous clay</td><td>10</td></tr>
<tr><td>L</td><td>Gravels, coarse sand, calc. clay</td><td>43</td><td colspan="2">Fluvimarine condition</td></tr>
<tr><td rowspan="2">L</td><td rowspan="2">Kurkar deposits</td><td>U</td><td>Sandstone, loamy sand (red bed)</td><td>20-30</td><td></td><td>Continental conditions, development of landmasses</td><td rowspan="2">Great upheaval movement in the end of Pliocene continuous to Pleistocene</td></tr>
<tr><td>L</td><td>Coarse to medium calcareous sandstone with occasionally content of shell fragment</td><td>5-40</td><td>Subsurface (wells of the study area)</td><td>Marine condition</td></tr>
<tr><td rowspan="5">Tertiary</td><td rowspan="2">Pliocene</td><td>U</td><td colspan="3">Limestone with pebbles, cobbles, gravel of chert, coarse quartz grains and shell fragments</td><td>2-5</td><td rowspan="2">In Awlad Ali area (Surface)
In almost all wells (Subsurface)</td><td rowspan="2">Shallow marine and inner neritic to littoral environment</td><td rowspan="2">Submergence</td></tr>
<tr><td>L</td><td colspan="3">Yellow and grey sandy marl. salty and gypsiferrous form an isolated hill standing amidst the channel of Wadi El-Arish</td><td>20 (Surface)
300 (Subsurface)</td></tr>
<tr><td rowspan="3">Miocene</td><td>U</td><td colspan="3">Gypsum deposits</td><td>Few cms to 40m.</td><td>R3 El-Arish (Subsurface)
South Gabal Yelek (Surface)</td><td>Forming the ancestor of Wadi El-Arish</td><td>Upheaval</td></tr>
<tr><td>M</td><td rowspan="2" colspan="3">Dark green sticky clay</td><td rowspan="2">47 minimum</td><td rowspan="2">(Subsurface)
in many wells</td><td rowspan="2" colspan="2">Submergence</td></tr>
<tr><td>L</td></tr>
</table>

That is, the measurements become the coefficients in an expression whose graph is a periodic function. Plots of the Fourier series representations of the multivariate observations will be curves that can be visually grouped [11].

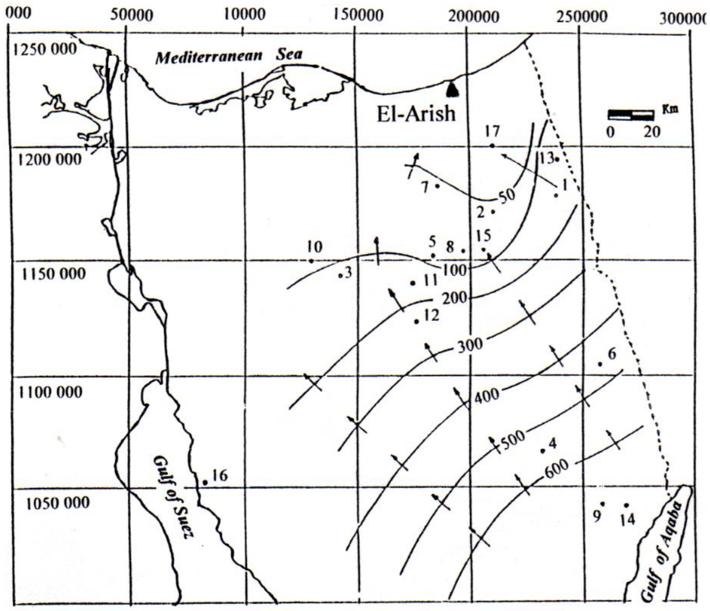

1- El-Qusaima,
2- El-Hodira,
3- El-Hamma,
4- El-Themd,
5- El-Hassana,
6- Kontella,
7- Libni,
8- El-Arish,
9- Sheira,
10- Gifgafa,
11- El-Arish-19,
12- Jica-17,
13- El-Amro,
14- Naqab,
15- Talet El-Buden,
16- Sudr.

Figure 1: Potentiometric surface map of the Upper Cretaceous aquifer.

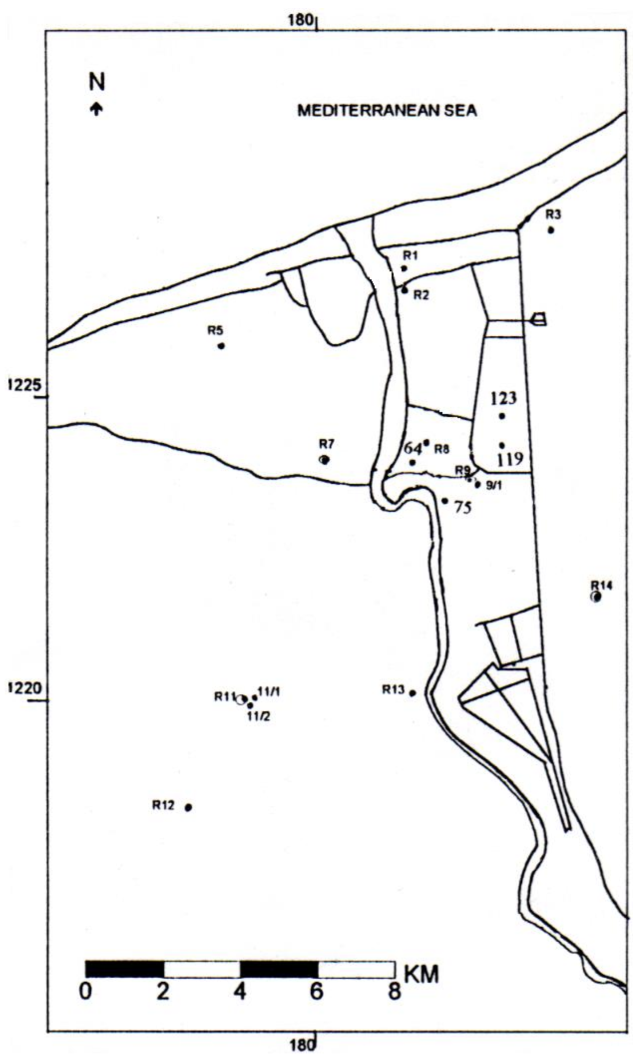

Figure 2: Location map of the Quaternary water wells in El Arish area.

Table 2: Hydrochemical data of the studied samples.

Well Name & No.	Anions (ppm)				Cations (ppm)				TDS	Formation
	HCO3-	SO4--	Cl-	CO3--	Mg^{++}	Ca^{++}	Na^{+}	K^{+}		
El-Qusima -	288	1300	2173	7.8	202	269	1450	6.3	5695	U.Cretaceous
El-Hodira -	308	509	672	4	78	80	600	7.8	2259	U.Cretaceous
El-Hamma -	144	1140	1749	-	104	246	1144	40	4567	U.Cretaceous
El-Themed -	183	279	217	12	46	96	115	4	982	U.Cretaceous
El-Hassana -	218	899	2174	-	181	261	1299	15	5047	U.Cretaceous
Kontella -	186	100	458	4	36	60	250	17	1112	U.Cretaceous
Libni-3 --	55	755	1900	-	47	480	943	26	4208	U.Cretaceous
El-Arish 15--	175	1585	2805	-	253	368	1751	10	6947	U.Cretaceous
Sheira2 –	99	410	274	-	82	22	223	14	1126	U.Cretaceous
Gifgafa –	432	494	2608	-	268	330	1065	34	5232	U.Cretaceous
ElArish19a—	85	439	1123	-	193	88	690	8	2626	U.Cretaceous
ElArish19b—	100	147	830	-	6	84	555	21	1744	U.Cretaceous
Jica 17 –	285	56	2852	-	103	130	1996	-	5420	U.Cretaceous
R1 ---	146	1001	792	-	216	65	552	13	2785	Quaternary
R2 ---	183	827	740	-	196	51	409	23	2429	Quaternary
R3 ---	220	134	728	-	37	19	520	11	1669	Quaternary
R7 ---	146	121	305	-	24	21	230	16	863	Quaternary
R8 ---	149	1028	785	-	196	53	612	14	2837	Quaternary
R9 ---	176	1200	1191	-	169	82	982	20	3822	Quaternary
R11 ---	386	956	1397	-	244	97	920	16	4016	Quaternary
R12 ---	231	994	802	-	64	59	886	13	3049	Quaternary
R13 ---	207	258	547	-	73	32	368	20	1505	Quaternary
R14 ---	323	1507	1420	-	326	30	1093	20	4718	Quaternary

- after Abdel Baki (1996) -- after JICA (1992) --- after RIWR (1993)

The application of finite Fourier series on the Upper Cretaceous and Quaternary groundwater samples is plotted in Figures (**3** and **4**), where all samples of the Upper Cretaceous aquifer have the same waveform pattern

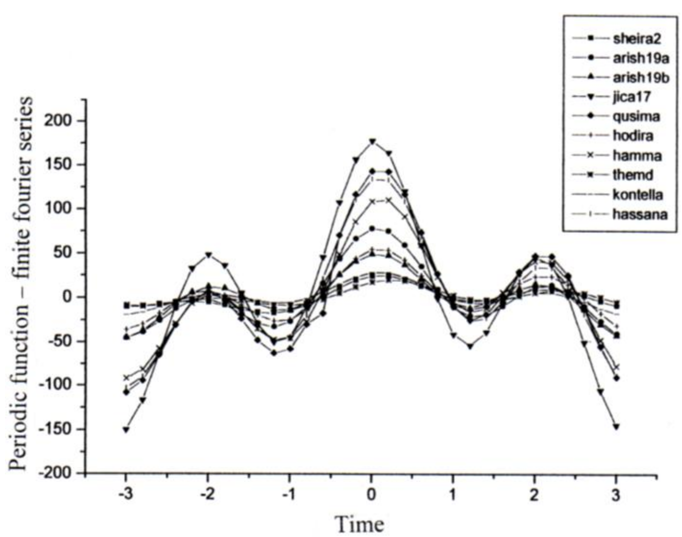

Figure 3: Andrews plots of Upper Cretaceous groundwater samples.

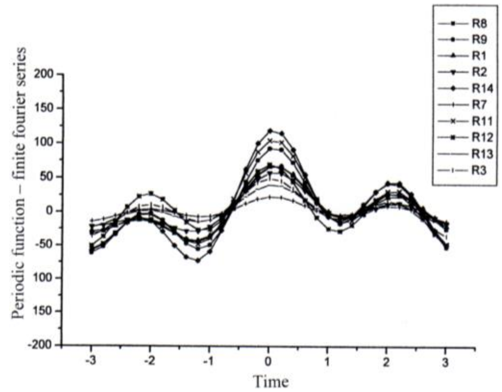

Figure 4: Andrews plots of Quaternary groundwater samples.

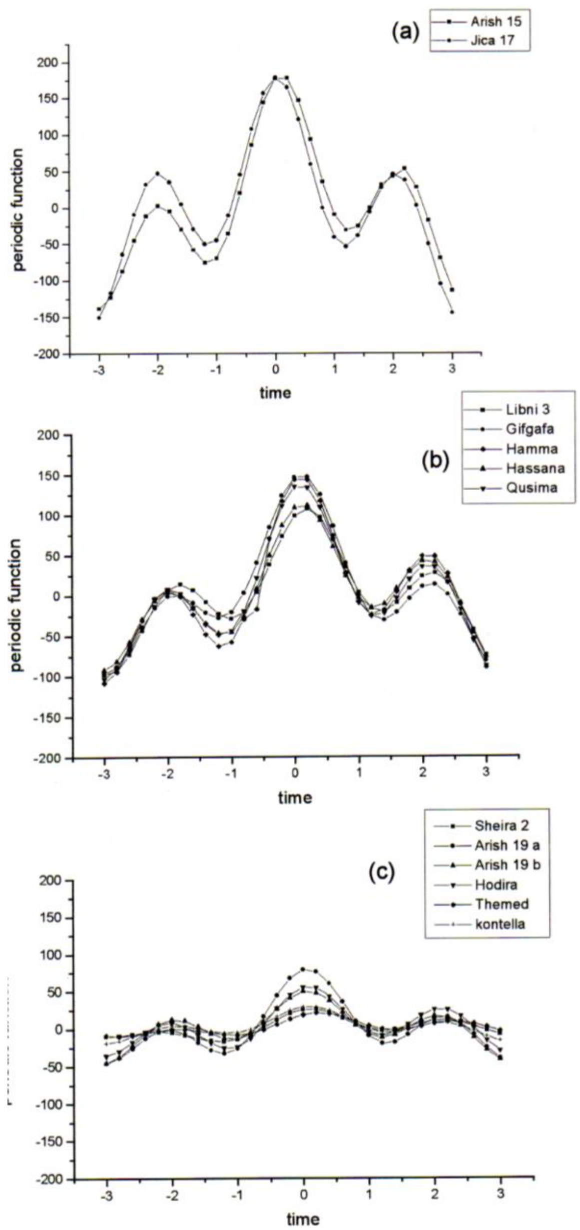

Figure 5: Different amplitudes of Upper Cretaceous water.

with different amplitudes. They are classified into high, middle, and low amplitude in Figure **5** (a, b, and c, respectively). The correlation between different amplitudes and the TDS value of every sample indicates that as the salinity increase, the amplitude increases. The same waveform pattern characterizes Quaternary groundwater samples as in the Upper Cretaceous aquifer with little difference in amplitude.

A complete agreement between the three groups resulted from Andrews plotting and Stiff diagram of the Upper Cretaceous water in Figure **6** (a, b, and c, respectively), where all samples have the same ionic water type Cl, SO4, HCO3, Na+K, Mg, Ca with a little exception in samples of El Hamma, Libni-3, El Arish19b, and El Themd, where they have Ca more than Mg.

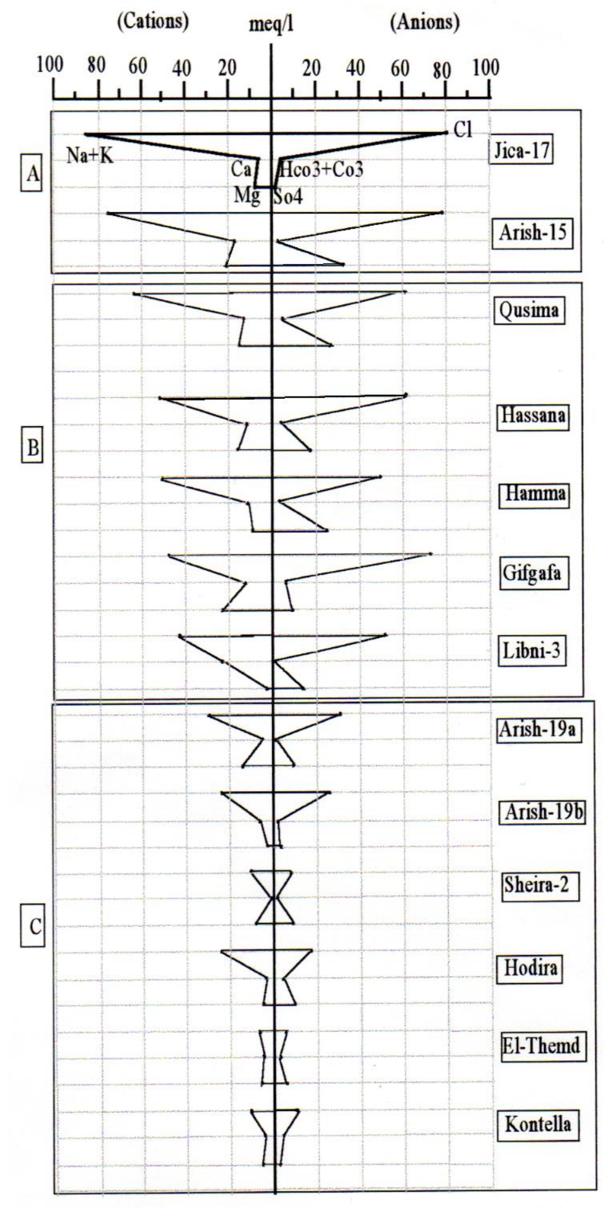

Figure 6: Stiff diagram of Upper Cretaceous water.

Applying the Stiff diagram for Quaternary water (Figure **7**) emphasized the same water type of Upper Cretaceous. This similarity is also reflected in Andrews plots in Figures (**3**) and (**4**).

Conclusion

According to the present study, Andrews plots succeeded to a large degree in illustrating and classifying groundwater samples in both Quaternary and Upper Cretaceous aquifers. The same waveform pattern

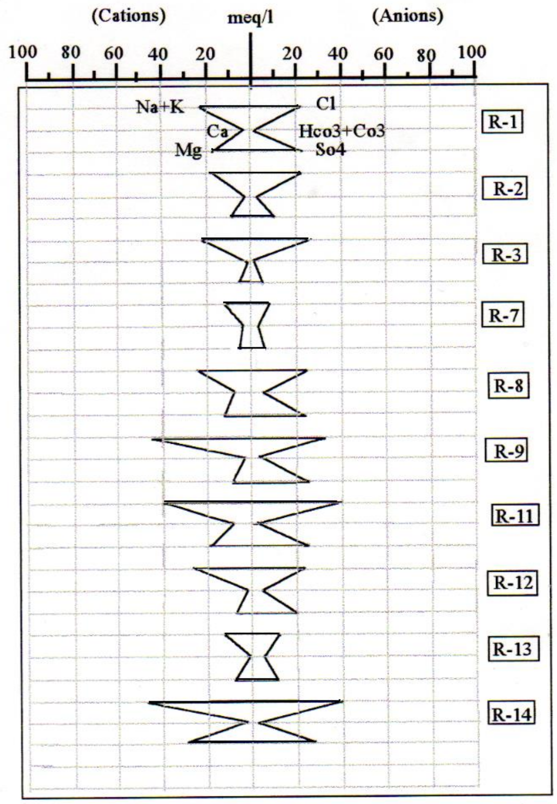

Figure 7: Stiff diagram of Quaternary water.

characterizes quaternary groundwater samples as in the Upper Cretaceous aquifer with little difference in amplitude. The similarity in the waveform pattern reflects the similarity in the chemical composition. This result is confirmed by the comparison with the Stiff conventional diagrams. This agreement between the two groundwater types suggests a hydraulic connection and mixing between the Quaternary and the Upper Cretaceous aquifers. It is worth mentioning that the Quaternary aquifer is in the most active valley in Northern Sinai and is subjected to a very high extraction rate. In addition, the Upper Cretaceous aquifer is confined and is subjected to potentiometric pressure. The mixing between Quaternary and Upper Cretaceous aquifers is confirmed by the radiocarbon age estimated by [12]. The estimated radiocarbon ages of groundwater samples in the delta Wadi El Arish range from 900 to 8800 Y.B.P. Also, Tritium dating refers to mixing between modern to sub-modern (old) age.

As a result, transforming the chemical composition of groundwater samples as a set of multivariate data to a waveform pattern as the Andrews plot is a practical statistical application for visual grouping and classification of groundwater samples.

References

[1] Abdel Baki AA. Hydrogeology of Carbonate aquifers in the central northeast Sinai. Bul Fac Sci., Assuit Univ. 1996; 25(I-F): pp. 45-67.

[2] Anderson TW. An introduction to multivariate statistical analysis, third edition. Wiley, 2003; pp 713.ISBN 0-471-36091-0.

[3] Boonprong S, Cao C, Torteeka P, Chen W. A Novel Classification Technique of Landsat-8 OLI Image-Based Data Visualization: The Application of Andrews' Plots and Fuzzy Evidential Reasoning, Remote Sensing, V. 2017; 9: p. 427. https://doi.org/10.3390/rs9050427

[4] Brown CE. Applied multivariate statistics in geohydrology and related sciences. Springer Berlin, Heidelberg, 1998; pp 248, ISBN: 978-3-642-80328-4. https://doi.org/10.1007/978-3-642-80328-4_1

[5] Dames, Moor Sinai development study, Phase I, Water resources, 1984; Vol. II (A and B).

[6] Fout N, Ma KL. Reliable Visualization: Verification of Visualization based on Uncertainty Analysis. Los Angeles: Tech. rep., University of California. – Davis 2012.

[7] García-Osorio C, Fyfe C. Visualization of High-Dimensional Data via Orthogonal Curves. J Univers Comput Sci. 2005; 11(11): 1806-1819.

[8] Gomaa MA. Hydrogeological and hydrochemical studies on Wadi El Arish, North Sinai, Egypt. M.Sc. Geol. Fac. Sci. Zagazig Univ. 1984.

[9] Jica. North Sinai Groundwater resources study in the Arab Republic of Egypt, final report. 1992.

[10] Jobson JD. Applied multivariate data analysis, 1992; V. 2: springer, New York. https://doi.org/10.1007/978-1-4612-0921-8

[11] Johnson RA, Wichern DW. Applied multivariate statistical analysis. 3rd Ed. 1992; Prentice-Hall international Inc.

[12] Khalil MA. Hydrogeological and geophysical investigation of the groundwater salinity problem in Northern Sinai-Peninsula Ph.D. JLU, Germany. 2002.

[13] Khattree R, Naik DN. Andrews plots for multivariate data: some new suggestions and applications, J Statist Plann Inferen, 2002; V. 100, (Issue 2): P. 411-425. https://doi.org/10.1016/S0378-3758(01)00150-1

[14] RIWR, BRGM. Sinai water resources study, phase II, final report. 1993; Pp.67.

[15] Steinberg DM. Robust design: experiments for improving quality, in Ghosh, S., and Rao, C, R., (Eds.), Handbook of Statistics, Vol. 13, North-Holland, Amsterdam, 1996; pp. 199-240. https://doi.org/10.1016/S0169-7161(96)13009-1